Dalton Transactions

A heterometallic macrocycle as a redox-controlled molecular hinge

Journal:	*Dalton Transactions*
Manuscript ID:	DT-ART-10-2014-003331.R1
Article Type:	Paper
Date Submitted by the Author:	09-Dec-2014
Complete List of Authors:	Severin, Kay; Ecole Polytechnique Federale de Lausanne, Institut de Chimie Moleculaire et Biologique Schouwey, Clément; EPFL, Scopelliti, Rosario; Ecole Polytechnique Federale de Lausanne, Institut des Sciences et Ingénierie Chimiques; Papmeyer, Marcus; EPFL,

Dalton Transactions RSCPublishing

Paper

A heterometallic macrocycle as a redox-controlled molecular hinge

Cite this: DOI: 10.1039/x0xx00000x

Clément Schouwey,[a] Marcus Papmeyer, Rosario Scopelliti[a] and Kay Severin[a]*

Received 00th January 2012,
Accepted 00th January 2012

DOI: 10.1039/x0xx00000x

www.rsc.org/

The ability to modify the structure of nanoscopic assemblies in a controlled fashion is an important prerequisite for the creation of functional supramolecular systems. Here, we describe a heterometallic Pt_2Cu_2-macrocycle which behaves as a molecular hinge. A square-planar Pt(II) complex with pendent 2-formylpyridine groups was synthesized and structurally characterized. Condensation of the complex with benzylamine followed by reaction with $Cu(MeCN)_4(BF_4)$ resulted in the formation of a rectangular Pt_2Cu_2-macrocycle. Upon chemical oxidation of the Cu centres, the macrocycle folds up to adopt a butterfly-like geometry in which the Pt centres approach each other. This process can be reversed by chemical reduction.

Introduction

The term "molecular machine" describes molecules or molecular assemblies which are able, upon receiving a stimulus, to transition between two or more structural states in order to achieve functionality.[1] Nature displays elegant examples of such systems, many of them being essential parts of living systems, such as kinesins, ATP-synthase and ion pumps.[2] The complexity and efficiency of these biological molecular machines is far ahead of what has been achieved in synthetic systems, but artificial molecular machines are becoming more and more sophisticated and interesting applications start to emerge.[1-3]

One can distinguish between two different classes of molecular machines, namely molecular motors and switches. According to definitions offered by Leigh *et al.*, "Returning a molecular-level switch to its original position undoes any mechanical effect it has on an external system..." whereas "when the components of a rotary motor return to their original position through a different pathway to the one they left by […], a physical task performed by the machine is not inherently undone...".[1] Therefore, although both classes of machines are able to influence their surroundings as a function of state, only a molecular motor can drive a system away from equilibrium.

Molecular hinges are systems in which molecular arms can move with respect to a central axis. Over the last years, a number of synthetic molecular hinges have been reported.[4] The hinge motion can rely on the intrinsic conformational flexibility of the molecule (e.g. rotation around the Cp-Fe-Cp axis of 1,1'-substituted ferrocenes),[4b,e] or it can be the result of an external chemical or physical stimulus.. It should be noted that molecular hinges are sometimes classified as scissors[5] or tweezers[6] However, not every molecular tweezer is a hinge, because the term tweezer has also been used for structurally rigid molecules and for molecules lacking a defined hinge axis.[7]

Below we describe the synthesis of a heterometallic Pt_2Cu_2-macrocycle. The macrocycle can undergo a reversible hinge motion which is controlled by the redox state of the Cu centres.

Results and Discussion

We have recently described the synthesis of molecular cages using metal-ligand interactions in combination with dynamic covalent imine bonds.[8] Expanding on this work, we were interested in synthesizing new metal-based building blocks with pendent formyl groups for subsequent reaction with amines. We therefore decided to prepare complex **3**, which displays two formyl groups oriented at 90° to each other. The formyl groups are situated in 2-position on a pyridine ring. This 2-formylpyridine motif is known to form potent bidentate binding site for transition metal cations upon reaction with amines.[9]

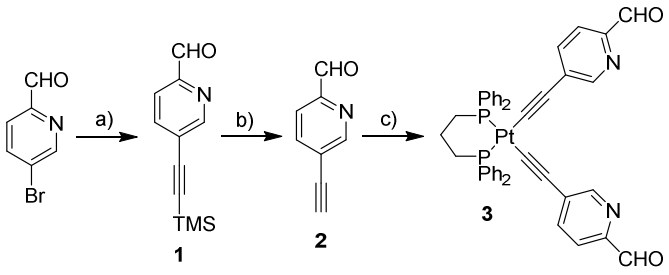

Scheme 1. Synthesis of complex **3**. Reagents and conditions: a) trimethylsylilacetylene, CuI, $Pd(PPh_3)_4$, NEt_3, 73%; b) K_2CO_3, MeOH 63%; c) $(dppp)PtCl_2$, CuI, THF/Et_2NH 9:1, 68%.

Complex **3** was synthesized in 3 steps and 31% overall yield starting from commercially available 5-bromo-2-pyridinecarboxaldehyde (Scheme 1). Its structure was

confirmed by multinuclear NMR spectroscopy, high-resolution ESI$^+$ mass spectrometry, elemental analysis, and single crystal X-ray diffraction. The crystallographic analysis confirmed the expected square planar structure of the complex (Fig. 1). However, although the C-Pt-C angle measures 89.1°, the angle $C_{carbonyl}$-Pt-$C_{carbonyl}$ deviates with 96.7 ° significantly from the expected 90° due to one ligand being significantly bent. This discrepancy demonstrates that complex **3** exhibits some geometrical flexibility.

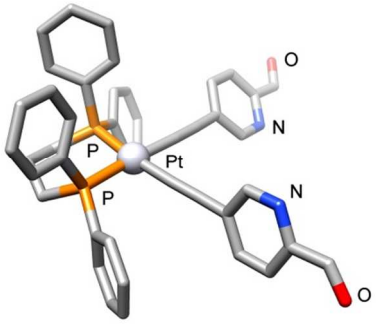

Fig. 1. Molecular structure of complex **3** in the solid state. Hydrogen atoms and solvent molecules are omitted for clarity.

Reaction of complex **3** with two equivalents of benzylamine in a mixture of dichloromethane and methanol (1:1) resulted in the formation of complex **4** (Scheme 2). The condensation product precipitated as a pale yellow powder upon concentration of the solution under vacuum at room temperature, and was isolated in 79% yield by filtration. In the solid state, complex **4** is stable under air for more than a week. However, long-term exposure to air will result in partial hydrolysis, and **4** should therefore be kept under an inert atmosphere if it is to be stored for longer periods of time. NMR and ESI$^+$-MS data, as well as elemental analysis of the complex all matched the structure depicted in Scheme 2.

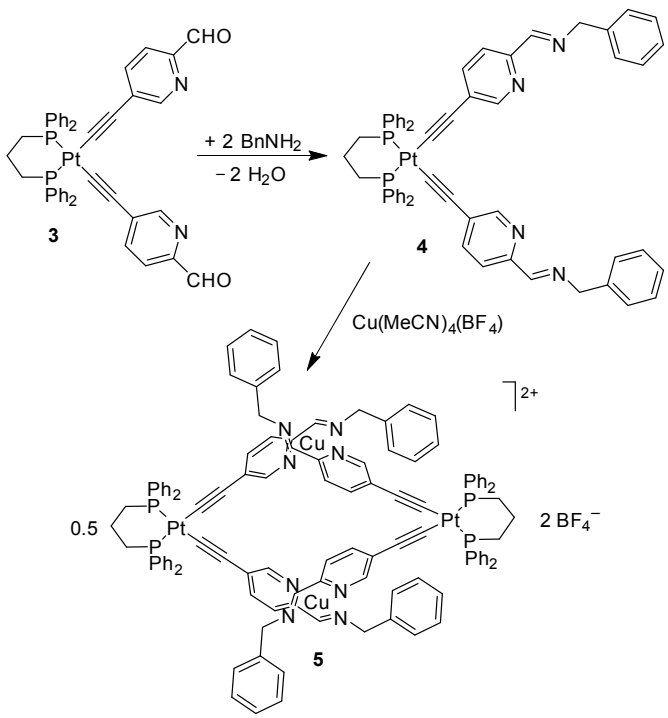

Scheme 2. Synthesis of complex **4** and **5**.

Complex **4** displays two binding sites suitable for coordination of metal ions. Reaction of equimolar amounts of complex **4** and $Cu(MeCN)_4BF_4$ in CD_2Cl_2 resulted in a deep red solution, indicative of the coordination of Cu^I at the 2-iminopyridine binding site. The ^{1}H NMR spectrum of the solution showed signals corresponding to the formation of a main, well-defined product **5** (Fig. 2).

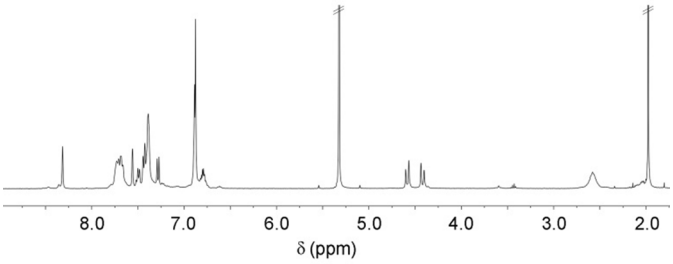

Fig. 2. ^{1}H NMR spectrum of an equimolar solution of complex **4** and $Cu(MeCN)_4BF_4$ in CD_2Cl_2.

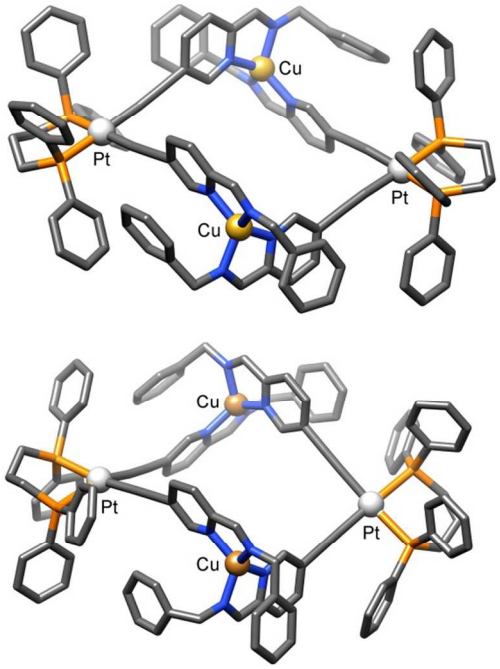

Fig. 3. Two possible structures of the cation of complex **5** as determined by molecular mechanics simulations. The *meso* form is shown on top and the *helicate* form on the bottom. Hydrogen atoms are omitted for clarity. Color code: gray C, blue N, orange P, white sphere Pt, brass sphere Cu.

High-resolution ESI+ mass spectrometry indicates that the main product of the reaction, complex **5**, has the composition $[(\mathbf{4})_2Cu_2]^{2+}$. DOSY NMR measurements of a solution of complex **5** in CD_2Cl_2 revealed the presence of a single species with a diffusion coefficient of 570 (± 5) $\mu m^2 s^1$, corresponding to a sphere with a radius of 9 Å according to the Stokes-Einstein equation. This value is in good agreement with the size of complex **5**, which was estimated by molecular mechanics simulations (the distance of the central carbon atoms in the

dppp ligands on opposite sides of the square is ~ 20Å). According to the molecular mechanics simulations, two structures are possible for complex **5**: a *meso* form and a *helicate* form (Fig. 3). We were not able to determine which one is the main product.

Attempts to isolate complex **5** by concentration of the solution under vacuum or by addition of Et_2O resulted in a red precipitate, which turned out to be insoluble in common organic solvents. Possibly, complex **5** is in equilibrium with oligomeric species that precipitate selectively upon isolation.

Greenish crystals suitable for X-ray diffraction, along with a red precipitate, were obtained by slow vapour diffusion of Et_2O in a red solution of complex **5** in $CHCl_3$/MeOH. The green colour of the crystals is indicative of the presence of Cu^{II}. Indeed, X-ray analysis revealed the formation of the bimetallic Cu^{II} complex **6** (Scheme 3 and Fig. 4). Complex **6** is composed of two **4** units linked by trigonal bipyramidal Cu^{II} centers, with a chloride ligand occupying the fifth coordination site of the Cu centres. The trigonal bipyramidal geometry of the two Cu^{II} ions brings the two **4** units in close proximity to each other, with a Pt···Pt distance of 7.84 Å.

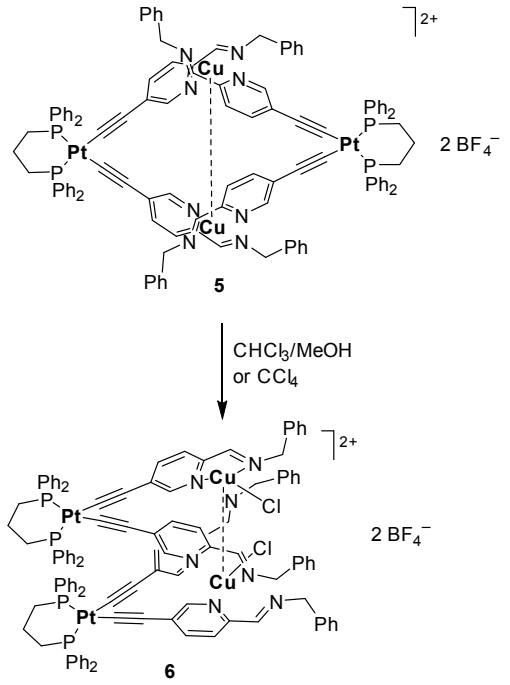

Scheme 3. Synthesis of complex **6** from **5** upon slow crystallization from $CHCl_3$/MeOH or by addition of CCl_4.

Complex **6** is likely formed by oxidation of **5** via chlorine atom transfer from $CHCl_3$. Indeed, Cu(I) complexes are known to catalyse atom transfer radical reactions of chlorinated substrates, where one of the key steps involves the homolytic cleavage of a carbon-chloride bond and the concomitant formation of a Cu(II)−Cl complex.[10] The assumption of a solvent-based oxidation was supported by the observation that the rate of the oxidation was strongly dependent on the nature of the chlorinated solvent. Solutions of **5** in CH_2Cl_2 were found to be stable over several weeks, whereas solutions of **5** in $CHCl_3$ turned green over a few days, and dissolution of **5** in CCl_4 resulted in the immediate formation of a greenish precipitate. The rates correlate with the relative homolytic dissociation energy of the first C-Cl bond of each solvent.[11]

The reaction of complex **5** with CCl_4 can be used to synthesize complex **6** on a preparative scale. After addition of CCl_4 to a solution of **5** in dichloromethane, complex **6** precipitates as a greenish amorphous powder in 91% yield upon concentration and addition of Et_2O. High-resolution ESI^+-MS data and the elemental analysis of the compound are in line with the structure determined by X-ray crystallography.

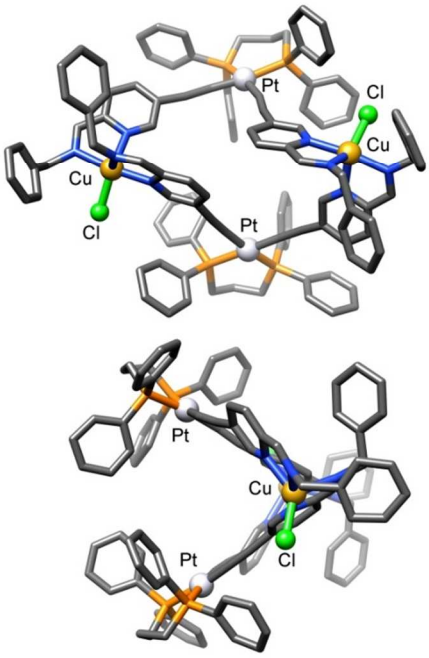

Fig. 4. Structure of complex **6** in the solid state. Color code: gray C, blue N, orange P, green sphere Cl, white sphere Pt, brass sphere Cu. Hydrogen atoms, solvent molecules and counter ions are omitted for clarity.

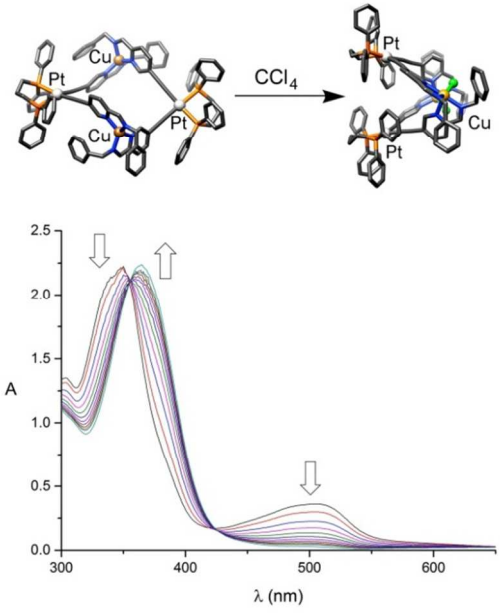

Fig. 5. Evolution of the UV-VIS spectrum of a solution of complex **5** in CH_2Cl_2 (2.39 μM) after addition of 2 eq. of CCl_4. Spectra were recorded every 10 min.

The oxidation of complex **5** to **6** can be performed in a controlled fashion. Addition of two equivalents of CCl_4 to a solution of complex **5** in CD_2Cl_2 (4.1 mM) resulted, over the course of 3 h, in the disappearance of the well-defined signals of **5** and the formation of new, broad signals corresponding to the paramagnetic species **6**. The oxidation of complex **5** to **6** also causes a significant change of the solution's colour, from deep red to greenish yellow, allowing the reaction to be monitored by UV-VIS spectroscopy (Fig. 5). Complex **5** displays two absorbance maxima at 350 and 504 nm, while complex **6** displays one maximum at 363 nm. During the oxidation of complex **5** to **6**, two isosbestic points are observed at 355 and 423 nm, indicative of a clean conversion.

The reverse reaction is also possible. Stirring a solution of complex **6** in CD_2Cl_2 for 2 days over activated Mg resulted in a change in the colour of the solution from greenish yellow to deep red. After removal of the Mg by filtration, the ^{1}H NMR spectrum of the solution was very similar to the one of freshly prepared **5**. The presence of complex **5** as a main product of the reaction was additionally confirmed by ESI$^+$-MS. The MS analysis also indicated the presence of minor amounts of side-products resulting from the cleavage of the Pt-alkyne bond. Alternatively, the conversion of complex **6** into **5** can be performed by successive de-metallation by extraction with aqueous NH_3 (25%)[12] and re-metallation with $Cu(MeCN)_4BF_4$. In this case, the ^{1}H NMR spectrum of the obtained solution was identical to the one of freshly prepared **5** and no side-products were observed. While the process can be reversed chemically, cyclic voltammetry measurements of complex **5** (0.1 M nBu$_4$NPF$_6$ in CH_2Cl_2) showed only a broad irreversible oxidation process centered at $E^0 = 0.881$ V.

Conclusions

A heterometallic Pt_2Cu_2-macrocycle was synthesized in a step-wise fashion using metal-ligand interactions and dynamic covalent imine bonds. Upon oxidation of the two Cu(I) sites with $CHCl_3$ or CCl_4, the macrocycle undergoes a hinge motion along the axis defined by the redox-active Cu centres. During this geometrical change, an extended rectangular structure with a Pt···Pt distance of around 12 Å is converted into a folded, butterfly-like structure with a Pt···Pt distance of 7.84 Å. The oxidation, and thus the hinge motion, can be reversed by reduction with Mg. A cleaner chemical "reset" can be achieved by a de-metallation/re-metallation step.

There is ample precedence for the utilization of Cu(I)/Cu(II) complexes with N-donor ligands in redox-controlled nanostructures.[1,3,13] Frequently, the interconversion between Cu(I) and Cu(II) is mediated electrochemically and the structural change is associated with a ligand exchange reaction of the chelating N-donor ligands. Our chemically induced oxidation by chlorine atom transfer does not involve a ligand exchange reaction but rather an expansion of the coordination number from four to five by addition of the chlorine atom. We have demonstrated the utility of this switch in a molecular hinge, but it appears likely that this motif can also be used for other adaptive molecular nanostructures.

Experimental section

General: Unless stated otherwise, all reactions were performed under a dry nitrogen atmosphere using standard Schlenk techniques. Solvents were dried using a solvent purification system from Innovative Technologies Inc. All commercially available chemicals were reagent grade and used without further purification. ^{1}H, ^{13}C and ^{31}P NMR spectra were recorded on a Bruker Avance III spectrometer (^{1}H: 400 MHz, ^{13}C: 100.6 MHz, ^{31}P: 161 MHz). Additional ^{1}H and ^{13}C spectra were recorded on a Bruker AvanceIII HD spectrometer (^{1}H: 600 MHz, ^{13}C: 150 MHz). Multiplicities of ^{13}C signals were determined by HSQC experiments. All chemical shifts are reported in ppm and referenced to residual solvent peak (^{1}H, ^{13}C) or H_3PO_4 (^{31}P) as external standards. Combustion analyses were performed with a Thermo Scientific Flash 2000 Organic Elemental Analyzer. Mass spectra were recorded with a Waters Q-TOF Ultima (ESI-TOF) or a LTQ-FT-Orbitrap-MS (nanoESI-Orbitrap) spectrometer. Melting points were measured in open-end capillary tubes with a melting point instrument (Edmund Bühler Sp6). UV-VIS spectra were recorded on a Varian Cary 50 bio spectrometer.
Cyclic voltammetry measurements were performed in CH_2Cl_2 (5 ml) containing nBu$_4$NPF$_6$ as electrolyte (0.1 M) to which 5 mg of freshly prepared complex **5** in CH_2Cl_2 (0.5 ml) were added. The scans were performed with a scan rate of 50 mV/s in a window from −0.6V to 1.2V with a graphite working electrode, a platinum counter electrode and an $Ag/AgNO_3$ pseudo-reference electrode. The electric potentials were referenced to the ferrocene/ferrocenium couple in order to determine the potential versus SHE.

Synthesis of 5-((trimethylsilyl)ethynyl)picolinaldehyde (1): Adapted from a reported procedure.[14] Trimethylsilylacetylene (3.2 g, 4.6 ml, 32 mmol) was added to a degassed solution of 5-bromopicolinaldehyde (2.0 g, 11 mmol) in toluene-NEt_3 3:1 (320 ml) and N_2 was bubbled into the solution for 5 min. $Pd(PPh_3)_4$ (300 mg, 260 μmol) and CuI (300 mg, 1.58 mmol) were added and the solution was degassed again, then stirred 2 h at room temperature. The solvent was removed under vacuum and the solid residue was dissolved in DCM (100 ml). The solution was washed with NH_4Cl (aq., sat., 50 ml) and brine (50 ml), dried over Na_2SO_4 and the solvent was removed under reduced pressure. Purification by column chromatography (SiO_2, DCM) afforded **2** (1.6 g, 73%) as a white solid. M.p. 73−76°C; ^{1}H NMR (400 MHz, $CDCl_3$): $\delta = 0.29$ (s, 9H), 7.81−7.96 (m, 2H), 8.81 (t, $J = 1.4$ Hz, 1H), 10.06 (s, 1H); ^{13}C NMR (100 MHz, $CDCl_3$): $\delta = -0.17$ (CH_3), 100.80 (C≡C), 102.87 (C≡C), 120.99 (C_{arom}), 124.81 (C_{arom}), 139.91 (C_{arom}), 151.17 (C_{arom}), 152.99 (C_{arom}), 192.69 (CHO); HRMS (ESI$^+$): m/z = 204.0849 $[M + H]^+$; calcd. for $[C_{11}H_{13}NOSi + H]^+$: 204.084.

Synthesis of 5-ethynylpicolinaldehyde (2): A solution of **2** (720 mg, 3.54 mmol) and K_2CO_3 (40 mg, 290 μmol) in MeOH (50 ml) was stirred for 2 h. The solvent was removed under vacuum and the solid residue was suspended in H_2O (20 ml), filtered, washed with H_2O (2 x 10 ml), and dried under vacuum to afford **3** (293 mg, 63%) as a brownish amorphous powder. M.p. 112−116°C; ^{1}H NMR (400 MHz, $CDCl_3$): $\delta = 3.43$ (s, 1H), 7.92-7.95 (m, 2H), 8.86 (t, $J = 1.5$ Hz, 1H), 10.08 (s, 1H); ^{13}C NMR (100 MHz, $CDCl_3$): $\delta = 79.87$ (C≡C), 84.20 (C≡C), 121.01 (C_{arom}), 123.77 (C_{arom}), 140.26 (C_{arom}), 151.59 (C_{arom}), 153.18 (C_{arom}), 192.65 (CHO); HRMS (ESI$^+$): m/z = 132.0454 $[M + H]^+$; calcd. for $[C_8H_5NO + H]^+$ 132.0449.

Synthesis of complex 3: A solution of (dppp)$PtCl_2$[15] (600 mg, 884 μmol), **3** (233 mg, 1.77 mmol), CuI (18.0 mg, 90.7 μmol) and Et_2NH (12 ml) in dry THF (100 ml) was stirred overnight at room temperature. The solvent was removed under reduced pressure and the residue was purified by column chromatography (SiO_2, DCM/EtOAc, 4:1) to afford **3** (522 mg, 68%) as a pale yellow

microcrystalline solid. M.p. 249−263 (dec.); ^{1}H NMR (400 MHz, CD_2Cl_2): δ = 1.86−2.21 (m, 2H), 2.45-2.69 (m, 4H), 7.19 (ddd, J = 8.0 Hz, J = 2.0 Hz, J = 0.9 Hz, 2H), 7.33−7.52 (m, 12H), 7.62 (dd, J = 8.1 Hz, J = 0.9 Hz, 2H), 7.68−7.76 (m, 8H), 8.06 (dd, J = 1.9 Hz, J = 0.9 Hz, 1H), 9.88 (d, J = 0.8 Hz, 1H); ^{13}C NMR (100 MHz, CD_2Cl_2): δ = 19.80 (CH_2), 25.69 (CH_2), 120.49 (CH), 128.47 (t, J = 5.4 Hz, CH), 128.92 (C_q), 130.42 (d, J = 58.3 Hz, C_q), 130.92 (CH), 133.01−133.91 (m, CH), 138.09 (CH), 148.79 (C_q), 152.13 (CH), 192.68 (CHO); ^{31}P NMR (162 MHz, CD_2Cl_2): −6.94 (t, $^1J_{P\text{-}Pt}$ = 1092.7 Hz); HRMS (ESI$^+$): m/z = 868.1848 $[M + H]^+$; calcd. for $[C_{43}H_{34}N_2O_2P_2Pt + H]^+$: 868.1826; anal. calcd. (%) for $C_{43}H_{34}N_2O_2P_2Pt$ (868.79): C 59.52, H 3.95, N 3.23; found: C 59.24, H 3.68, N 2.99. Single crystals of **3** were obtained by slow vapour diffusion of EtOAc into a solution of **3** in DCM/MeOH (95:5).

Synthesis of complex 4: A solution of complex **3** (250 mg, 288 µmol) and benzylamine (62 mg, 64 µl, 580 µmol) in DCM-MeOH 1:1 (40 ml) was stirred overnight at room temperature. The solution was concentrated adiabatically under vacuum to ~ 10 ml. The resulting precipitate was collected by centrifugation, washed with MeOH (2 x 2 ml) and Et_2O (2 x 2 ml), and dried under vacuum to afford complex **4** (239 mg, 79%) as a pale yellow amorphous powder. M.p. 208−213 (dec.); ^{1}H NMR (400 MHz, CD_2Cl_2): δ = 1.95−2.15 (m, 2H), 2.50−2.65 (m, 4H), 4.77 (d, J = 1.5 Hz, 4H), 7.07 (ddd, J = 8.3 Hz, J = 2.1 Hz, J = 0.7 Hz, 2H), 7.21−7.27 (m, 2H), 7.29−7.35 (m, 4H), 7.35−7.47 (m, 12H), 7.69−7.77 (m, 8H), 7.96 (dd, J = 2.0 Hz, J = 0.9 Hz, 2H), 8.33 (app br q, J = 1.2 Hz, 2H); ^{13}C NMR (100 MHz, CD_2Cl_2): δ = 20.04 (CH_2), 25.50−26.10 (m, CH_2), 64.98 (CH_2), 106.40−106.80 (m, C_q), 113.87 (d, J = 146.1 Hz, C_q), 119.79 (CH), 125.81 (CH), 127.05 (CH), 128.19 (CH), 128.43-128.71 (m, CH), 130.94 (CH), 130.97 (m, C_q), 132.82−134.65 (m, CH), 138.17 (CH), 139.49 (C_q), 150.70 (C_q), 151.51 (CH), 162.81 (CH); ^{31}P NMR (162 MHz, CD_2Cl_2): δ = −6.80 (t, $^1J_{P\text{-}Pt}$ = 1092.5 Hz); HRMS (ESI$^+$): m/z = 1046.3049 $[M + H]^+$; calcd. for $[C_{57}H_{48}N_4P_2Pt + H]^+$: 1046.3085; anal. calcd. (%) for $C_{57}H_{48}N_4P_2Pt$ (1046.07): C 65.45, H 4.63, N 5.36; found C 65.15, H 4.50, N 4.97.

Synthesis of complex 5: $Cu(MeCN)_4BF_4$ (1.6 mg, 4.9 µmol) was added to a solution of complex **4** (5.0 mg, 4.9 µmol) in CD_2Cl_2 (0.6 ml) under air and the resulting solution was analyzed. ^{1}H NMR (400 MHz, CD_2Cl_2): δ = 1.87−2.10 (m, 2H), 2.50−2.67 (m, 4H), 4.42 (d, ^2J = 14.4 Hz, 2H), 4.58 (d, ^2J = 13.8 Hz, 2H), 6.66−6.77 (m, 2H), 6.77-6.93 (m, 8H), 7.26 (d, J = 8.1 Hz, 2H), 7.30−7.48 (m, 12H), 7.53 (d, J = 2.1 Hz, 2H), 7.58−7.82 (m, 8H), 8.30 (s, 2H); ^{13}C NMR (150 MHz, CD_2Cl_2): δ = 20.17 (CH_2), 25.60−26.00 (m, CH_2), 64.05 (CH_2), 105.90-106.30 (m, C_q), 118.40-119.90 (m, C_q), 117.12 (CH), 125.85 (CH), 128.44 (C_q), 128.71 (CH), 128.97−129.16 (m, CH)), 129.34 (CH), 131.57 (d, J = 12.6 Hz, CH), 132.80−134.20 (m, C_q), 134.01 (dt, J = 60.0 Hz, J = 5.2 Hz, CH), 137.56 (C_q), 138.64 (CH), 146.31 (C_q), 151.19 (CH), 159.40 (CH); ^{31}P NMR (162 MHz, CD_2Cl_2): δ = −6.99 (t, $^1J_{P\text{-}Pt}$ = 1094.3 Hz); HRMS (ESI$^+$): m/z = 1109.2312 $[M - 2(BF_4)]^{2+}$; calcd. for $[C_{114}H_{96}Cu_2N_8P_4Pt_2]^{2+}$: 1109.2336.

Synthesis of complex 6: CCl_4 (1 ml) was added to a solution of $Cu(MeCN)_4BF_4$ (12.0 mg, 38.2 µmol) and **4** (40.0 mg, 38.2 µmol) in DCM (10 ml) under air. The solution was stirred for 2 h and then concentrated under vacuum to ~ 5 ml. Et_2O (10 ml) was added, causing the formation of a greenish precipitate, which was isolated by centrifugation, washed with Et_2O (3 x 5 ml), and dried under vacuum to afford complex **6** (43.0 mg, 91%) as a greenish amorphous powder. HRMS (ESI$^+$): m/z = 1144.6964 $[M - 2(BF_4)]^{2+}$; calcd. for $[C_{114}H_{96}Cl_2Cu_2N_8P_4Pt_2]^{2+}$: 1144.6989; anal. calcd. (%) for $C_{114}H_{96}Cl_2Cu_2N_8P_4Pt_2B_2F_8{\cdot}CH_2Cl_2$ (2548.67): C 54.20, H 3.88, N 4.40; found: C 53.96, H 3.77, N 4.20.

Reduction of complex 6 to complex 5 with Mg: Mg (5 mg, 206 µmol) was suspended in a solution of complex **6** (5.0 mg, 2.0 µmol) in CD_2Cl_2 and the solution was vigorously stirred for 1 h. Mg was removed by filtration and the solution was analysed by ^{1}H NMR spectroscopy and high-resolution ESI$^+$-MS.

Reduction of complex 6 to complex 5 by de-metallation and re-metallation:[12] A solution of complex **6** (5 mg, 2.03 µmol) in CD_2Cl_2 (1 ml) was extracted with 25% aqueous NH_3 (1 ml). The organic phase was washed with H_2O (5 x 1 ml), then $Cu(MeCN)_4BF_4$ (1.28 mg, 4.06 µmol) was added and the solution was analysed by ^{1}H NMR spectroscopy.

X-Ray crystallography: The data collection for complex **3** was performed at room temperature using Cu K_α radiation on an Agilent Technologies SuperNova dual system in combination with an Atlas CCD detector. The diffraction data of complex **6** were measured at 100(2) using Mo K_α radiation on a Bruker APEX II CCD diffractometer equipped with a kappa geometry goniometer. The dataset for complex **6** were reduced by EvalCCD[16] and then corrected for absorption.[17] The data reduction for complex **3** was carried out by Crysalis PRO.[18] The solutions and refinements were performed by SHELX.[19] The crystal structures were refined using full-matrix least-squares based on F^2 with all non hydrogen atoms anisotropically defined. Hydrogen atoms were placed in calculated positions by means of the "riding" model. The refinement of the crystal structure of compound **6** was difficult because of the weakness of the measured sample. The data were cut at the resolution of 0.98 Å and several restraints and constraints were applied to the final model. A large number of phenyl rings was treated by restraining their C-C distances and by flattening the entire ring (SADI and FLAT cards). The anisotropic refinement of all light atoms (B, C, N, F) was restrained by means of the SIMU cards and to prevent becoming non-positive definite, some of them (C16, C17, C130, C131, C156, C157) were constrained using the EADP card. The geometry of three out of four BF_4^- was restrained to be almost tetrahedral using the DFIX card applied to B-F bond distances and F...F lengths. Crystallographic data (excluding structure factors) for the structures reported in this paper have been deposited at the Cambridge Crystallographic Data Center (CCDC) as Supplementary Publication No. CCDC 1031450 (**3**) and 1031451 (**6**). Copies of the data can be obtained free of charge on application to the CCDC, 12 Union Road, Cambridge, CB2 1EZ, U.K. (fax, (internat.) +44-1223-336033; E-mail, deposit@ccdc.cam.ac.uk).

Acknowledgements

This work was supported by funding from the Swiss National Science Foundation and by the Ecole Polytechnique Fédérale de Lausanne (EPFL). Molecular graphics and analyses were performed with the UCSF Chimera package. Chimera is developed by the Resource for Biocomputing, Visualization, and Informatics at the University of California, San Francisco (supported by NIGMS P41-GM103311).[20] We thank Yeon-Ji Oh and Carlos Gilberto Morales Guio for help with cyclic voltammetry measurements.

Notes and references

[a] *Institut des Sciences et Ingénierie Chimiques*
Ecole Polytechnique Fédérale de Lausanne (EPFL)
1015 Lausanne (Switzerland)

Fax: (+41) 21-693-9305
E-mail: kay.severin@epfl.ch

1 E. R. Kay, D. A. Leigh and F. Zerbetto, *Angew. Chem. Int. Ed.*, 2007, **46**, 72.
2 M. Schliwa, *Molecular Motors*; Wiley-VCH, Weinheim, 2003.
3 Reviews: (*a*) P. Ceroni, A. Credi and M. Venturi, *Chem. Soc. Rev.*, 2014, **43**, 4068; (*b*) X. Yan, B, Zheng and F. Huang, *Polymer Chem.*, 2013, **4**, 2395; (*c*) W. Yang, Y. Li, H. Liu, L. Chi and Y. Li, *Small*, 2012, **8**, 504; (*d*) A. Coskun, M. Babaszak, R. D. Astumian, J. F. Stoddart and B. A. Grzybowski, *Chem. Soc. Rev.*, 2012, **41**, 19; (*e*) V. Balzani, A. Credi and M. Venturi, *Chem. Soc. Rev.*, 2009, **38**, 1542; (*f*) V. Balzani, A. Credi and M. Venturi, *ChemPhysChem*, 2008, **9**, 202; (*g*) W. R. Browne and B. L. Feringa, *Nature Nanotech.*, 2006, **1**, 25.
4 Examples: (*a*) R. Nandy and S. Sankararaman, *Org. Biomol. Chem.*, 2010, **8**, 2260; (*b*) I. Baumgardt and H. Butenschön, *Eur. J. Org. Chem.*, 2010, 1076; (*c*) C.-K. Koo, K.-L. Wong, K.-C. Lau, W.-Y. Wong and M. H.-W. Lam, *Chem. Eur. J.*, 2009, **15**, 7689; (*d*) S. Ernst and G. Haberhauer, *Chem. Eur. J.*, 2009, **15**, 13406; (*e*) D. Huber, H. Hubner and P. Gmeiner, *J. Med. Chem.*, 2009, **52**, 6860; (*f*) G. Haberhauer, *Angew. Chem. Int. Ed.*, 2008, **47**, 3635; (*g*) S. Sankararaman, G. Venkataramana and B. Varghese, *J. Org. Chem.*, 2008, **73**, 2404; (*h*) R. Nandy, M. Subramoni, B. Varghese and S. Sankararaman, *J. Org. Chem.*, 2007, **72**, 938; (*i*) C.-K. Koo, B. Lam, S.-K. Leung, M. H.-W. Lam and W.-Y. Wong, *J. Am. Chem. Soc.*, 2006, **128**, 16434; (*j*) Y. Norikane and N. Tamaoki, *Org. Lett.*, 2004, **6**, 2595.
5 (*a*) K. Tanaka and K. Kinbara, *Mol. BioSyst.*, 2008, **4**, 512; (*b*) T. Muraoka, K. Kinbara and T. Aida, *Chem. Commun.*, 2007, 1441; (*c*) T. Muraoka, K. Kinbara, Y. Kobayashi and T. Aida, *J. Am. Chem. Soc.*, 2003, **125**, 5612.
6 Examples: (*a*) R. B. Murphy, D.-T. Pham, S. F. Lincoln and M. R. Johnston, *Eur. J. Org. Chem.*, 2013, 2985; (*b*) H. Yoon, C.-H. Lee and W.-D. Jang, *Chem. Eur. J.*, 2012, **18**, 12479; (*c*) G. Chen, S. Bouzan and Y. Zhao, *Tetrahedron Lett.*, 2010, **51**, 6552; (*d*) C.-H. Lee, H. Yoon and W.-D. Jang, *Chem. Eur. J.*, 2009, **15**, 9972;
7 Reviews: (*a*) J. Leblond and A. Petitjean, *ChemPhysChem*, 2011, **12**, 1043; (*b*) M. Hardouin-Lerouge, P. Hudhomme and M. Sallé, *Chem. Soc. Rev.*, 2011, **40**, 30; (*c*) F.-G. Klärner and B. Kahlert, *Acc. Chem. Res.*, 2003, **36**, 919.
8 (*a*) C. Schouwey, R. Scopelliti and K. Severin, *Chem. Eur. J.*, 2013, **19**, 6274; (*b*) A. Granzhan, C. Schouwey, T. Riis-Johannessen, R. Scopelliti and K. Severin, *J. Am. Chem. Soc.*, 2011, **133**, 7106; (*c*) A. Granzhan, T. Riis-Johannessen, R. Scopelliti and K. Severin, *Angew. Chem. Int. Ed.*, 2010, **49**, 5515.
9 T. K. Ronson, S. Zarra, S. P. Black and J. R. Nitschke, *Chem. Commun.*, 2013, **49**, 2476.
10 W. T. Eckenhoff and T. Pintauer, *Catal. Rev.*, 2010, **52**, 1.
11 P. Goldfinger and G. Martens, *Trans. Faraday Soc.* 1961, **57**, 2220.
12 J. D. Megiatto Jr. and D. I. Schuster, *Org. Lett.*, 2011, **13**, 1808.
13 Review: (*a*) M. Boiocchi and L. Fabbrizzi, *Chem. Soc. Rev.*, 2014, **43**, 1835. (*b*) J.-P. Collin, V. Heitz and J.-P. Sauvage, *Top. Curr. Chem*., 2005, **262**, 29.
14 J.-F. Ayme, J. E. Beves, D. A. Leigh, R. T. McBurney, K. Rissanen and D. Schultz, *Nature Chem.*, 2012, **4**, 15.
15 N. C. Dopke and H. E. Oemke, *Inorg. Chim. Acta*, 2011, **376**, 638.
16 A. J. M. Duisenberg, L. M. J. Kroon-Batenburg and A. M. M. Schreurs, *J. Appl. Crystallogr.*, 2003, **36**, 220.
17 R. H. Blessing, *Acta Crystallogr. A*, 1995, **51**, 33.
18 *Crysalis PRO*, Agilent Technologies, release 1.171.37.31, 2014.
19 G. M. Sheldrick, *Acta Crystallogr. A*, 2008, **64**, 112.
20 E. F. Petersen, T. D. Goddard, C. C. Huang, G. S. Couch, D. M. Greenblatt, E. C. Meng and T. E. Ferrin, *J. Comput. Chem.*, 2004, **13**, 1605.

Graphic for the TOC

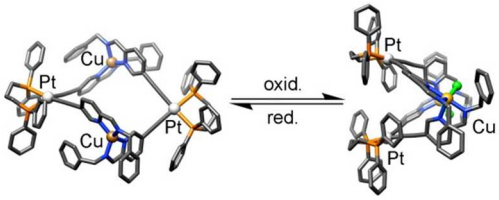

Text for the TOC: The geometry of a heterometallic Pt-Cu macrocycle is controlled by the redox state of the Cu centres. An elongated form with a long Pt···Pt distance is observed for Cu(I), whereas a folded form with a short Pt···Pt distance is found for Cu(II).